

Dinitrosyl Iron Complexes (DNICs) Bearing O-Bound Nitrito Ligand:  
Reversible Transformation between the Six-Coordinate  $\{\text{Fe}(\text{NO})_2\}^9$   
[[1-Melm) $_2(\eta^2\text{-ONO})\text{Fe}(\text{NO})_2$ ] ( $g = 2.013$ ) and Four-Coordinate  $\{\text{Fe}(\text{NO})_2\}^9$   
[[1-Melm)(ONO)Fe(NO) $_2$ ] ( $g = 2.03$ )

Fu-Te Tsai,<sup>†</sup> Ting-Shen Kuo,<sup>‡</sup> and Wen-Feng Liaw<sup>\*†</sup>

Department of Chemistry, National Tsing Hua University, Hsinchu, Taiwan, and Department of Chemistry,  
National Taiwan Normal University, Taipei, Taiwan

Received November 14, 2008; E-mail: wfliaw@mx.nthu.edu.tw

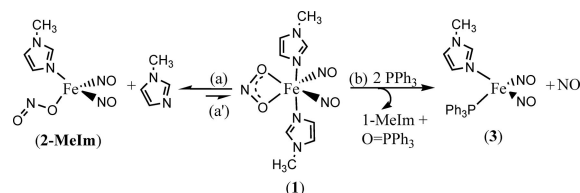
Dinitrosyl iron complexes (DNICs), one of the possible forms for storage and transport of NO, have been known to exert NO bioactivity under physiological and pathological conditions.<sup>1,2</sup> It is proposed that DNICs play a crucial role in regulating iron uptake/storage, triggering the expression of proteins against nitrosative stress, and reassembling [Fe–S] clusters after nitrosative damage.<sup>3</sup> Characterization of DNICs in vitro/vivo has been made possible via the distinct EPR signal at  $g = 2.03$ .<sup>1–3</sup> Nitrite, an ubiquitous molecule in vivo, particularly in the endocrine system, serves in intravascular NO storage/transport in blood circulation.<sup>4</sup> Nitrite signaling operates through the cooperative action with hemes, thiols, amines, polyphenols, and ascorbate yielding nitric oxide during physiological and pathological hypoxia.<sup>5a</sup> In particular, the biotransformation of nitroglycerin (GTN) in the presence of cysteine/NADH generating NO and nitrite was proposed to proceed via the nitrite-containing ferrous intermediate (Supporting Information (SI) Scheme S1).<sup>5b</sup>

DNICs containing the various ligation modes [S,S]/[S,O]/[S,N]/[N,N] were recently synthesized.<sup>6</sup> In spite of the few O-bound monodentate nitrito/chelating nitrito complexes such as *cis*-[Fe(NO)(NO<sub>2</sub>)(TC-5,5)] and [HB(3,5-Me<sub>2</sub>pz)<sub>3</sub>Fe( $\eta^2$ -ONO)Cl]<sup>–</sup> reported,<sup>7</sup> no discrete nitrite-containing DNICs are known. In this contribution, the temperature-dependent reversible transformation between the six-coordinate chelating nitrito  $\{\text{Fe}(\text{NO})_2\}^9$  DNIC [(1-Melm) $_2(\eta^2\text{-ONO})\text{Fe}(\text{NO})_2$ ] (1-Melm = 1-methylimidazole) (**1**) and the four-coordinate monodentate nitrito  $\{\text{Fe}(\text{NO})_2\}^9$  DNIC [(1-Melm)(ONO)Fe(NO) $_2$ ] (**2-Melm**) was demonstrated.<sup>8</sup> Transformation of an O-bound nitrito ligand of complex **1** into NO promoted by PPh<sub>3</sub> accompanied by the formation of  $\{\text{Fe}(\text{NO})_2\}^{10}$  [(1-Melm)(PPh<sub>3</sub>)Fe(NO) $_2$ ] (**3**) was also elucidated.

Reaction of  $[\text{Fe}(\text{CO})_2(\text{NO})_2]^+$  with 1 equiv of  $[\text{NO}_2]^-$  and 2 equiv of 1-Melm in THF at  $-10^\circ\text{C}$  led to the isolation of the chelating nitrito  $\{\text{Fe}(\text{NO})_2\}^9$  [(1-Melm) $_2(\eta^2\text{-ONO})\text{Fe}(\text{NO})_2$ ] (**1**) characterized by IR (1749 vs 1820  $\text{cm}^{-1}$  (MeOH)) and EPR spectroscopies and single-crystal X-ray crystallography. In the isotopic labeling experiments, the IR spectrum of complex **1** exhibits a diagnostic  $\nu_{\text{O-N-O}}$  vibrational frequency of the bidentate nitrito ligand ( $^{15}\text{NO}_2^-$ ) at 1248  $\text{cm}^{-1}$ , shifting from 1261  $\text{cm}^{-1}$  (KBr).

The variable temperature EPR spectra demonstrate that the thermal transformation occurred between the neutral six-coordinate DNIC **1** and the neutral four-coordinate **2-Melm** in THF (Scheme 1a and 1a'). To corroborate the existence of **2-Melm**, the analogue [(HIm)(ONO)Fe(NO) $_2$ ] (HIm = imidazole) (**2-HIm**) was synthesized with IR  $\nu_{\text{NO}}$  stretching frequency 1729 vs 1800  $\text{cm}^{-1}$  (MeOH) and  $\nu_{\text{N-O}}$  of the O-bound nitrito 1269  $\text{cm}^{-1}$  (KBr,  $\nu^{15}\text{N-O}$

Scheme 1



1249  $\text{cm}^{-1}$ ). The variable temperature EPR spectrum of complex **2-HIm** displays a well-resolved nine-line hyperfine splitting with  $g = 2.031$  ( $a_{\text{NO}} = 2.60$  G and  $a_{\text{HIm}} = 4.81$  G) at 180 K (SI Figure S1). As shown in Figure 1a–b and also in SI Figure S2, EPR studies

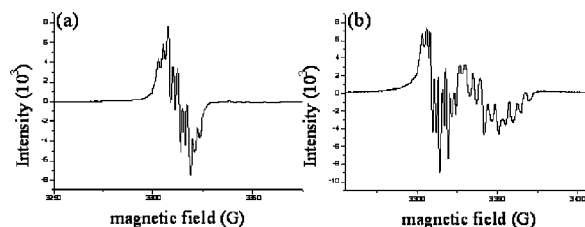


**Figure 1.** EPR spectra of the thermal transformation between complex **1** and **2-Melm** in THF solution at (a) 220 K (complex **2-Melm** ( $g_{\text{av}} = 2.031$ ,  $a_{\text{NO}} = 2.60$  G,  $a_{1\text{-Melm}} = 4.81$  G)), (b) 180 K (complex **1** ( $g_{\text{av}} = 2.013$ ,  $a_{\text{NO}} = 5.78$  G,  $a_{1\text{-Melm}} = 9.21$  G) and complex **2-Melm** ( $g_{\text{av}} = 2.031$ ,  $a_{\text{NO}} = 2.60$  G,  $a_{1\text{-Melm}} = 4.81$  G)).

were performed at 300, 220, 180, and 160 K for identification and detection of species formed via transformation of complex **1**. Complex **1** dissolved in THF exhibits a well-resolved nine-line hyperfine splitting with a  $g$  value of 2.031 at 220 K. This EPR spectrum, identical to the EPR spectrum of complex **2-HIm** characterized by single-crystal X-ray crystallography, indicates the formation of the four-coordinate complex **2-Melm**.<sup>9</sup> At 180 K, the EPR spectrum exhibits a well-resolved nine-line hyperfine splitting with a  $g$  value of 2.030 ( $a_{\text{NO}} = 2.60$  G and  $a_{1\text{-Melm}} = 4.81$  G) along with the appearance of a well-resolved thirteen-line hyperfine splitting with a  $g$  value of 2.013 ( $a_{\text{NO}} = 5.78$  G and  $a_{1\text{-Melm}} = 9.21$  G) assigned to the spectrum of complex **1** (Figure 1b). (Under the presence of 100-fold 1-Melm, the EPR spectrum of complex **1** displays a well-resolved thirteen-line hyperfine splitting with a  $g$  value of 2.013 in  $\text{CH}_2\text{Cl}_2$  at 180 K ( $a_{\text{NO}} = 5.11$  G and  $a_{1\text{-Melm}} = 8.63$  G) (SI Figure S3).) This result demonstrates that complexes **1** and **2-Melm** undergo a temperature-dependent reversible transformation (dynamic equilibrium).

Figure 2a and 2b display the thermal ellipsoid plots of the neutral complexes **1** and **2-HIm**, respectively, and the selected bond lengths and bond angles are given in the figure captions, respectively. It is

<sup>†</sup> National Tsing Hua University.

<sup>‡</sup> National Taiwan Normal University.

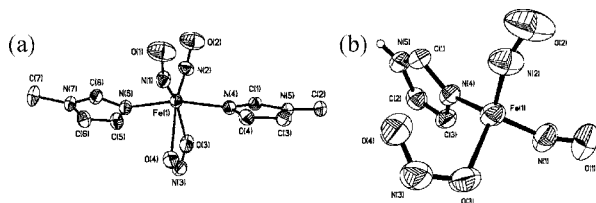


**Figure 2.** ORTEP drawing and labeling scheme of complexes **1** and **2-HIm** with thermal ellipsoids drawn at 50% probability. Selected bond lengths (Å) and angles (deg): (a) Fe(1)–N(1) 1.724(3), Fe(1)–N(2) 1.718(3), Fe(1)–N(4) 2.113(2), Fe(1)–N(6) 2.143(2), Fe(1)–O(3) 2.306(2), Fe(1)–O(4) 2.286(3), N(1)–O(1) 1.172(4), N(2)–O(2) 1.155(4), N(3)–O(3) 1.259(4), N(3)–O(4) 1.263(4); Fe(1)–N(1)–O(1) 149.3(3), Fe(1)–N(2)–O(2) 151.0(3), O(3)–Fe(1)–O(4) 54.31(10), O(3)–N(3)–O(4) 112.4(3). (b) Fe(1)–N(1) 1.692(3), Fe(1)–N(2) 1.681(3), Fe(1)–N(4) 2.007(2), Fe(1)–O(3) 1.992(2), N(1)–O(1) 1.173(4), N(2)–O(2) 1.171(4), N(3)–O(3) 1.284(4), N(3)–O(4) 1.206(4); Fe(1)–N(1)–O(1) 162.7(3), Fe(1)–N(2)–O(2) 163.6(3), O(3)–N(3)–O(4) 113.3(3).

noticed that the Fe(1)–N(1) and Fe(1)–N(2) bond lengths of 1.724(3) and 1.718(3) Å in complex **1**, respectively, are longer than the reported Fe–N(O) bond lengths ranging from 1.661(4) to 1.695(3) Å of {Fe(NO)<sub>2</sub>}<sup>9</sup> DNICs.<sup>6,9</sup> In contrast, the mean Fe–N(O) bond length of 1.685(3) Å (1.681(3) and 1.692(3) Å) in complex **2-HIm** falls in the range of the {Fe(NO)<sub>2</sub>}<sup>9</sup> DNICs.<sup>6,9</sup> Also, the Fe(1)–N(1)–O(1) and Fe(1)–N(2)–O(2) bond angles of 149.3(3)° and 151.0(3)° in complex **1** are smaller than those of the published four-coordinate DNICs ranging from 157.1(2)° to 172.1(3)°.<sup>6,9</sup> The (Fe)O(3)–N(3) bond length of 1.284(4) Å in the O-bound nitrito complex **2-HIm**, compared to those of 1.259(4) and 1.263(4) Å in complex **1**, is significantly longer than the distal N(3)–O(4) bond length of 1.206(4) Å.<sup>7b</sup>

To investigate the activation of nitrite yielding nitric oxide, reaction of complex **1** with 2 equiv of PPh<sub>3</sub> was conducted. In contrast to the inertness of complex **2-HIm** toward PPh<sub>3</sub>, addition of 2 equiv of PPh<sub>3</sub> into complex **1** promotes O-atom transfer of the chelating nitrito under mild conditions to generate OPPh<sub>3</sub> (<sup>31</sup>P NMR: δ = 29.2 ppm in CDCl<sub>3</sub>),<sup>10</sup> the neutral EPR-silent {Fe(NO)<sub>2</sub>}<sup>10</sup> [(1-MeIm)(PPh<sub>3</sub>)Fe(NO)<sub>2</sub>] (**3**) identified by IR and UV–vis spectroscopies and single-crystal X-ray crystallography (SI Figure S4), and the released NO trapped by [PPN]<sub>2</sub>[S<sub>5</sub>Fe(μ-S)<sub>2</sub>FeS<sub>5</sub>] generating the corresponding [PPN][S<sub>5</sub>Fe(NO)<sub>2</sub>] in THF–MeCN.<sup>9</sup> The mechanism of transformation of complex **1** into complex **3** can be rationalized as the following reaction sequences (SI Scheme S2); intermediate [(1-MeIm)<sub>2</sub>(NO)Fe(NO)<sub>2</sub>] (**A**) containing the nitroxyl anion (NO<sup>−</sup>) coordinated ligand (nitrite-to-nitroxyl conversion) was proposed to be produced upon O-atom transfer to PPh<sub>3</sub>, the sequential reductive elimination of NO, and the concomitant ligand substitution of 1-MeIm by PPh<sub>3</sub> yields complex **3**.

In summary, in contrast to tetrahedral {Fe(NO)<sub>2</sub>}<sup>9</sup> DNICs with an EPR *g* value of 2.03, the nonclassical six-coordinate {Fe(NO)<sub>2</sub>}<sup>9</sup> DNIC **1** displays an EPR signal *g* = 2.013. The temperature-dependent reversible transformation occurs between DNIC **1** and DNIC **2-MeIm**. The chelating nitrito of {Fe(NO)<sub>2</sub>}<sup>9</sup> DNIC **1**, triggered by PPh<sub>3</sub>, undergoes O-atom transfer to result in reductive

elimination of NO along with the generation of {Fe(NO)<sub>2</sub>}<sup>10</sup> DNIC **3**, in contrast to the inertness of the nitrite-containing {Fe(NO)<sub>2</sub>}<sup>9</sup> DNIC **2-HIm** toward PPh<sub>3</sub>. The findings, EPR signals of *g* = 2.013 for complex **1** and *g* = 2.03 for complexes **2-MeIm/2-HIm**, imply that characterization of DNICs in vitro/in vivo may be possible via their distinctive EPR signal *g* = 2.03 for the tetrahedral DNICs and EPR signal *g* = 2.01 for the six-coordinate DNICs. This result may signify that nitrite-containing {Fe(NO)<sub>2</sub>}<sup>9</sup> DNICs may serve as the transient intermediates for the conservation of NO bioactivity under biological conditions, and the nonclassical six-coordinate nitrite-containing {Fe(NO)<sub>2</sub>}<sup>9</sup> DNICs may act as an active center to trigger the transformation of nitrite into nitric oxide in biological systems.<sup>11</sup> Studies of the electronic structure and reactivity of complexes **1** and **2-HIm** are underway.

**Acknowledgment.** We gratefully acknowledge financial support from the National Science Council of Taiwan.

**Supporting Information Available:** X-ray crystallographic files in CIF format for the structure determinations of [(1-MeIm)<sub>2</sub>(η<sup>2</sup>-ON-O)Fe(NO)<sub>2</sub>], [(HIm)(ONO)Fe(NO)<sub>2</sub>], and [(1-MeIm)(PPh<sub>3</sub>)Fe(NO)<sub>2</sub>]. This material is available free of charge via the Internet at <http://pubs.acs.org>.

## References

- Bulter, A. R.; Megson, I. L. *Chem. Rev.* **2002**, *102*, 1155–1166.
- (a) Boese, M.; Keese, M. A.; Becker, K.; Busse, R.; Mulsch, A. *J. Biol. Chem.* **1997**, *272*, 21767–21773. (b) Cesareo, E.; Parker, L. J.; Pedersen, J. Z.; Nuccetelli, M.; Mazzetti, A. P.; Pastore, A.; Federici, G.; Caccuri, A. M.; Ricci, G.; Adam, J. J.; Parker, M. W.; Bello, M. L. *J. Biol. Chem.* **2005**, *280*, 42172–42180.
- (a) Lewandowska, H.; Męczyńska, S.; Sochanowicz, B.; Sadło, J.; Kruszewaj, M. *J. Biol. Inorg. Chem.* **2007**, *12*, 345–352. (b) Kim, S.; Ponka, P. *Proc. Natl. Acad. Sci. U.S.A.* **2002**, *99*, 12214–12219. (c) Sellers, V. M.; Johnson, M. K.; Dailey, H. A. *Biochemistry* **1996**, *35*, 2699–2704. (d) Yang, W.; Roger, P. A.; Ding, H. *J. Biol. Chem.* **2002**, *277*, 12868–12873. (e) D'Autréaux, B.; Horner, O.; Oddou, J.-L.; Jeandey, C.; Gambarelli, S.; Berthomieu, C.; Latour, J.-M.; Michaud-Soret, I. *J. Am. Chem. Soc.* **2004**, *126*, 6005–6016.
- Bryan, S. N.; Fernandez, O. B.; Bauer, M. S.; Garcia-Saura, F. M.; Milsom, B. A.; Rassaf, T.; Maloney, E. R.; Bharti, A.; Rodriguez, J.; Feilish, M. *Nat. Chem. Biol.* **2005**, *1*, 290–297.
- (a) Lundberg, J. O.; Weitzberg, E.; Gladwin, M. T. *Nat. Rev. Drug Discovery* **2008**, *7*, 156–167. (b) Artz, J. D.; Toader, V.; Zavorin, S. I.; Bennett, B. M.; Thatcher, G. R. J. *Biochemistry* **2001**, *40*, 9256–9264.
- (a) Huang, H.-W.; Tsou, C.-C.; Kuo, T.-S.; Liaw, W.-F. *Inorg. Chem.* **2008**, *47*, 2196–2204. (b) Tsai, M.-L.; Hsieh, C.-H.; Liaw, W.-F. *Inorg. Chem.* **2007**, *46*, 5110–5117. (c) Tsai, M.-L.; Liaw, W.-F. *Inorg. Chem.* **2006**, *45*, 6583–6585. (d) Hung, M.-C.; Tsai, M.-C.; Liaw, W.-F. *Inorg. Chem.* **2006**, *45*, 6041–6047.
- (a) Franz, K. J.; Lippard, S. J. *J. Am. Chem. Soc.* **1999**, *121*, 10504–10512. (b) Arulsamy, N.; Bohle, D. S.; Hansert, B.; Powell, A. K.; Thomson, A. J.; Wocadlo, S. *Inorg. Chem.* **1998**, *37*, 746–750.
- Enemark, J. H.; Feltham, R. D. *Coord. Chem. Rev.* **1974**, *13*, 339–406.
- (a) Tsou, C.-C.; Lu, T.-T.; Liaw, W.-F. *J. Am. Chem. Soc.* **2007**, *129*, 12626–12627. (b) Lu, T.-T.; Chiou, S.-J.; Chen, C.-Y.; Liaw, W.-F. *Inorg. Chem.* **2006**, *45*, 8799–8806. (c) Tsai, F.-T.; Chiou, S.-J.; Tsai, M.-C.; Tsai, M.-L.; Huang, H.-W.; Chiang, M.-H.; Liaw, W.-F. *Inorg. Chem.* **2005**, *44*, 5872–5881. (d) Tsai, M.-L.; Chen, C.-C.; Hsu, I.-J.; Ke, S.-C.; Hsieh, C.-H.; Chiang, K.-A.; Lee, G.-H.; Wang, Y.; Liaw, W.-F. *Inorg. Chem.* **2004**, *43*, 5159–5167.
- (a) Afshar, R. K.; Eroy-Reveles, A. A.; Olmstead, M. M.; Mascharak, P. K. *Inorg. Chem.* **2006**, *45*, 10347–10354. (b) Cheng, L.; Powell, D. R.; Khan, M. A.; Richter-Addo, G. B. *Chem. Commun.* **2000**, 2301–2302.
- Zweier, J. L.; Wang, P.; Samouilov, A.; Kuppusamy, P. *Nat. Med.* **1995**, *1*, 804–809.

JA808743G